Annex 1: Visualisation of the FMC procedure.

1. Failure Conditions

$$F_{\perp}^{\sigma} = \frac{I_2 + \sqrt{I_4}}{2\bar{R}_{\perp}^{t}} = 1 \qquad \text{IFF1 and IFF3}$$

$$F_{\perp}^{\tau} = (b_{\perp}^{\tau} - 1)\frac{I_2}{\bar{R}_{\perp}^{c}} + b_{\perp}^{\tau}\frac{\sqrt{I_4}}{\bar{R}_{\perp}^{c}} = 1 \quad \text{with}$$

$$I_2 = \sigma_2 + \sigma_3 \; ; \; I_4 = (\sigma_2 - \sigma_3)^2 + 4\tau_{23}^2 \; ;$$

$$b_{\perp}^{\tau} = \frac{1 + (\sigma_2^{c\tau} + \sigma_3^{c\tau})/\bar{R}_{\perp}^{c}}{(\sigma_2^{c\tau} + \sigma_3^{c\tau})/\bar{R}_{\perp}^{c} + \sqrt{(\sigma_2^{c\tau} - \sigma_3^{c\tau})^2} / \bar{R}_{\perp}^{c}} = 1.09$$

from calibration point □ (see figure)
$(\sigma_2^{c\tau}, \sigma_3^{c\tau})$ = *(-40 MPa, -191 MPa)* and
mean values $\bar{R}_{\perp}^{t} = 40MPa$, $\bar{R}_{\perp}^{c} = 144MPa$.

Test data for this quasi-isotropic plane (σ_2, σ_3) are assumed from isotropic knowledge.

Note: Inherent to the FMC is a ‘Mode Fit’. This fit needs less data then the usually applied ‘Global Fit’ (such as with Tsai/Wu) and maps the MfFD, additionally! Appropriate fictitious data set.

$b_{\perp}^{\tau} \geq 1$ means angle $\geq 45°$ (45° = zero friction).

2. Test Data Mapping = Modelling

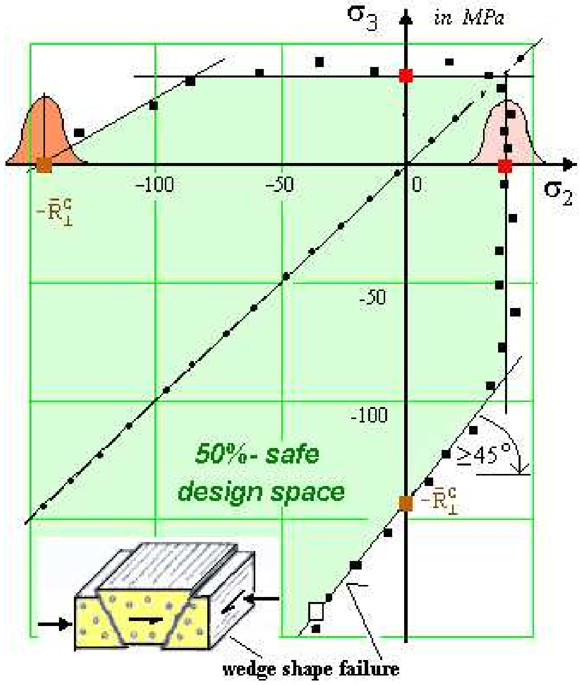

3. Rounding-off in MiFD, MfFD

$$\left(\frac{1}{f_{Res}^{(res)}}\right)^{\dot{m}} = \left(\frac{1}{f_{Res}^{\perp\sigma 2}}\right)^{\dot{m}} + \left(\frac{1}{f_{Res}^{\perp\tau}}\right)^{\dot{m}} + \left(\frac{1}{f^{\perp\sigma 3}}\right)^{\dot{m}}$$

Means $\bar{R}_{\perp}^{t}, \bar{R}_{\perp}^{c} \Rightarrow$ *Design Allowables* $R_{\perp}^{t}, R_{\perp}^{c}$,

$b_{\perp}^{\tau}$ remains because it is a physical property.

The mode reserve factors read (2D case)

$$f_{Res}^{\perp\sigma 2} = R_{\perp}^{t} / \sigma_2 \; , \; f_{Res}^{\perp\sigma 3} = R_{\perp}^{t} / \sigma_3 \; ,$$

$$f_{Res}^{\perp\tau} = R_{\perp}^{c} / (2b_{\perp}^{\tau}\sigma_2 - \sigma_2 - \sigma_3) \; .$$

* In the frame of an *automatic* numerical process a negative becoming f_{Res}^{mode} is set 10

* Automatic rounding without affecting adjacent modes.

4. "Design Curve"

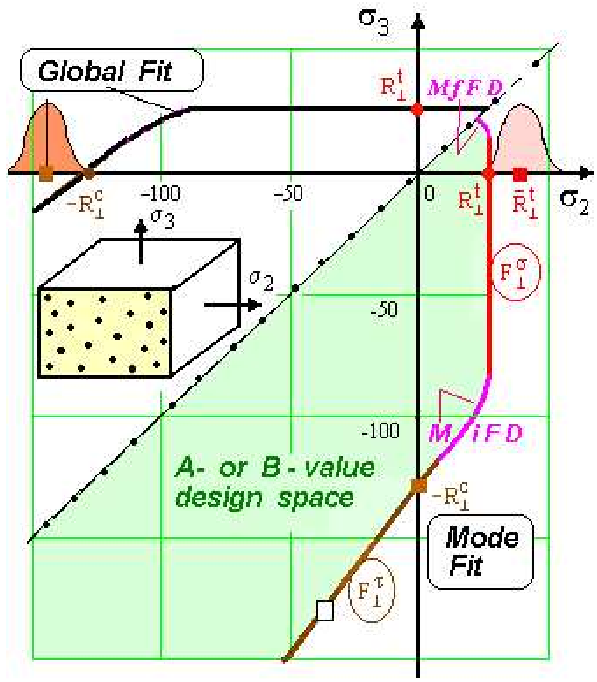

Figure A1: 2D case $\{\sigma\} = (0, \sigma_2, \sigma_3, 0, 0, 0)^T$.
MiFD:=Mixed Failure Domain, MfFD:= Multi-fold Failure Domain.
Both, MiFD and MfFD rounding-off is considered in the lower figure.

Annex 2: Determination of max $I_3^{3/2}$ (Query $F_{\perp\parallel}$ for the *case discrimination)*

A numerical problem exists with $F_{\perp\parallel}$ if $b_{\perp\parallel}(I_2 I_3 - I_5)$ becomes $-I_3^{3/2}$ in Eq(24d). Then, visualized in the 2D space by the $\tau_{21}(\sigma_2)$-curve in *Fig.***A2,** this curve turns asymptotically and an intersection with a proportional stress beam from the origin to determine $f_{\mathrm{Res}}^{\perp\parallel}$ is not achieved anymore. The reserve factor becomes indefinite and the effort imaginary. To generally bypass this difficulty one has to put a query in the program and replace, if applicable, the formulation of the asymptotically becoming curve by a limiting value $max\, I_3^{3/2}$. This is a 'horizontal' line in the 2D case of *Fig.A2*. Hence, the limit for the applicability of $F_{\perp\parallel}$ for the given *3D* state of stress (marked by a tilde sign) is $I_3^{3/2}/(I_2 I_3 - I_5) = -b_{\perp\parallel}$. In order to have a safe distance the parameter $b_{\perp\parallel}$ is increased by a very small factor χ. Setting into the failure condition $F_{\perp\parallel} = 1$, eqn(16), the new ratio $\max I_3^{3/2}/(\tilde{I}_2 \tilde{I}_3 - \tilde{I}_5) = -\chi \cdot b_{\perp\parallel}$ it can be deduced from $\max I_3^{3/2} + b_{\perp\parallel} \max I_3^{3/2}/(-\chi b_{\perp\parallel}) = \bar{R}_{\perp\parallel}^{3}$ a bound

$$\max I_3 = [\frac{\chi}{\chi - 1}]^{2/3} \cdot \bar{R}_{\perp\parallel}^{2} \quad \text{with} \quad \chi = 1.01 \quad \ldots\ldots \quad \text{3D case} \qquad \text{(A 1)}$$

$$\max tau = [\frac{\chi}{\chi - 1}]^{1/3} \cdot \bar{R}_{\perp\parallel} \quad , \quad \max I_3 = \max tau^2 \;, \quad \ldots\ldots \quad \text{2D case} \qquad \text{(A 2)}$$

In the 2D case the procedure can be visualized (see *Figure* **A2***)* by viewing at some distinct angles in the (τ_{21}, σ_2) graph. These are, employing the limiting beam $\frac{\tau_{21}}{-\sigma_2} = 2 \cdot b_{\perp\parallel}$, the radiant $\cot \Psi_{\max} = (\frac{\tau_{21}}{-\sigma_2})$ and the angle $\Psi°_{\max} = ar\cot(2b_{\perp\parallel}) \cdot 180/\pi$. To safely remain on the 'intersection side' a reduction of the angle $\Psi°_{\max}$ is introduced by the factor χ by setting $\Psi° = ar\cot(2\chi \cdot b_{\perp\parallel}) \cdot 180/\pi$. Hence, the sub-case of maxI3 is $\max tau = \frac{\bar{R}_{\perp\parallel}}{\sqrt[3]{1 - (2b_{\perp\parallel}/\cot\Psi)}}$ with $\cot\Psi = 2\chi b_{\perp\parallel}$. And the reserve factors become $f_{\mathrm{Res}}^{\perp\tau} = \frac{\bar{R}_{\perp}^{c}}{-\sigma_2}$, $f_{\mathrm{Res}}^{\perp\parallel} = \frac{\max tau}{|\tau_{21}|}$.

For the effort it is analogous.

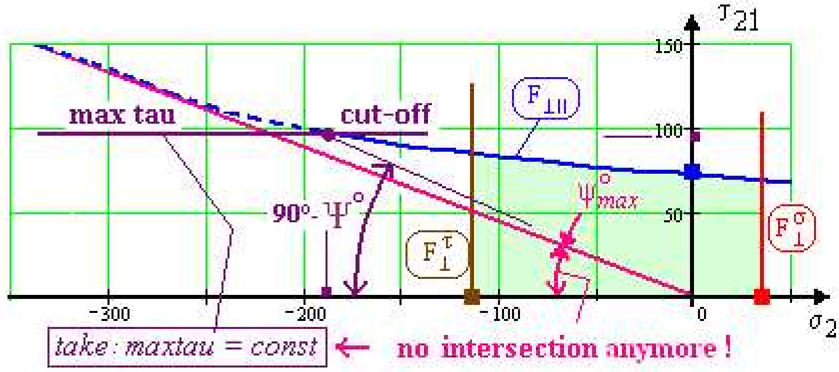

Fig.A2: Illustration of the cut-off in order to guarantee an intersection and to avoid imaginary or indefinite numbers. Eqs(1, 16), IFF2. (for Eq(30d) no inter-section problem anymore.)

Annex 3: Visualisation of Hardening and Softening

$$\gamma_{21} = \frac{\tau_{21}}{G_{\parallel\perp(0)}} + 0.002\left(\frac{\tau_{21}}{R^{\perp\parallel}_{p0.2}}\right)^{n_{\perp\parallel}}$$

calibration point =.strength point $\left(R_{\perp\parallel}\ ,\ \gamma_{pl}(R_{\perp\parallel})\right)$

$$\rightarrow n_{\perp\parallel} = \frac{\ln\left(\gamma_{pl}(R_{\perp\parallel})\right)}{\ln\left(R_{\perp\parallel}/R^{\perp\parallel}_{p0.2}\right)}$$

hardening

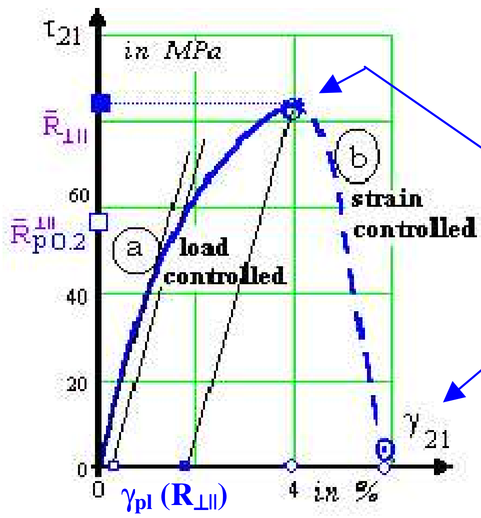

$$\tau^{(s)}_{21} = \frac{R_{\perp\parallel}}{1+\exp\dfrac{a^{\perp\parallel}_{s}\gamma_{21}}{b^{\perp\parallel}_{s}}}$$

calibration points:

$\left(0.99\ R_{\perp\parallel},\ \gamma_{21}(R_{\perp\parallel})\right)$ o

e.g. $\left(0.1R_{\perp\parallel},\ \gamma_{21}(0.1R_{\perp\parallel})\right)$

$\rightarrow a^{\perp\parallel}_{s},\ b^{\perp\parallel}_{s}$

softening

Fig.A3 : Measured shear stress – shear strain curves. Mapping by Eqns(19, 22a). Strain-controlled demands for stiff test frame. (bars to indicate mean or typical values are skipped in the windows here)

TableA3 : Definition of the various lamina types

I : Tensile coupon , *isolated* lamina, *load*-controlled → *weakest link type* test results
II : Tensile coupon , *isolated* lamina, *strain*-controlled (stiff test frame)
III: *Embedded (constraint)* lamina, *strain*-controlled → *redundant type* test results

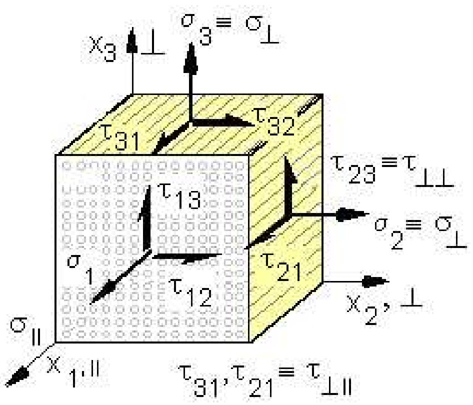

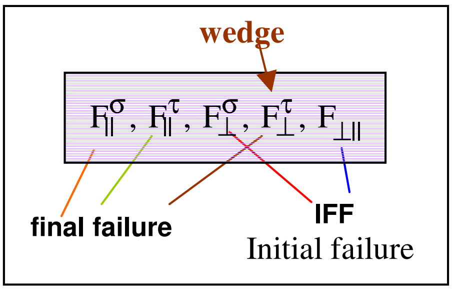

Fig. 1 : Failure criticality

$R^{t}_{\parallel}(=X^{t}), R^{c}_{\parallel}(=X^{c}), R_{\perp\parallel}(=S), R^{t}_{\perp}(=Y^{t}), R^{c}_{\perp}(=Y^{c});$

$E_{\parallel}, E_{\perp}, G_{\parallel\perp}, \nu_{\perp\parallel}, \nu_{\perp\perp}$

$\{\sigma\}=(\sigma_{1},\sigma_{2},\sigma_{3},\tau_{23},\tau_{13},\tau_{12})^{T}$

Fig.2a. UD lamina. Stress and strength notations of 3D state of stress. t: = tension, c: = compression.

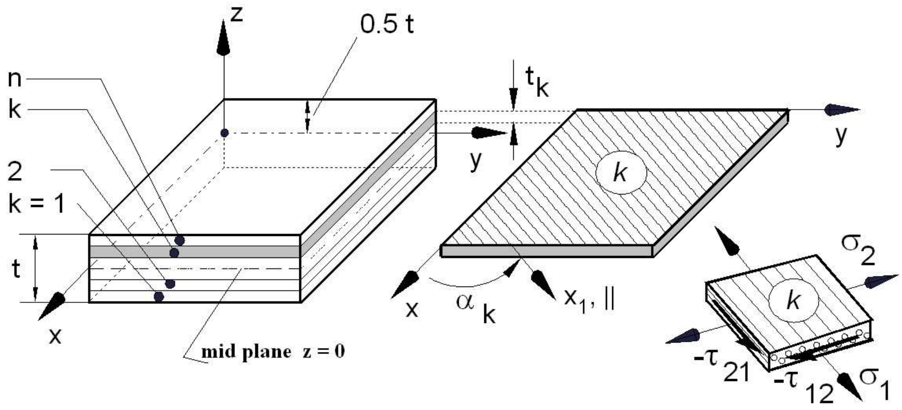

Fig. 2b. Laminate and k' th lamina subjected to a plane state of stress (mid-plane z = 0)

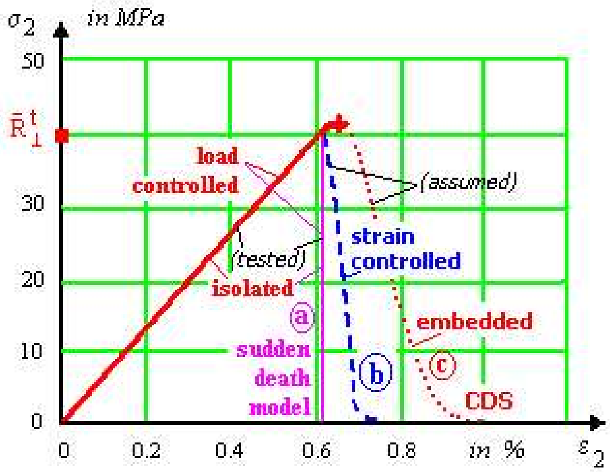

Fig. 3. The differences in the stress-strain beha - viour of isolated and embedded UD-laminae. For the (b)- and (c)-curve the Eq(22) is applied. The softening parameters for (b) and (c) are diffe- rent. Due to embedding, point + higher than ■)

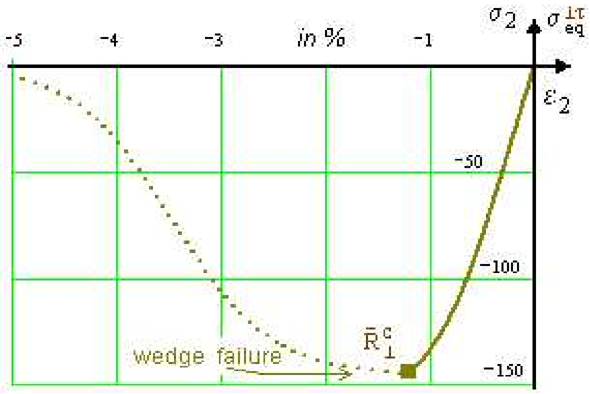

Fig. 4. Transversally compr. stress-strain curve $\sigma_2^c(\varepsilon_2)$; UD-lamina (softening parameters are assumed).GFRP: E-glass/MY750/ HY917/DY063[3]. $\bar{E}^c_{\perp 0} = 16.2\ GPa;\ a_s^{\perp c} = -3.45\,\%,\ b_s^{\perp c} = 0.47\,\%$, $n^{\perp c} = 6.6$. $\{\bar{R}\} = (1280,\ 800,\ 40,\ 145,\ 73)^T$.

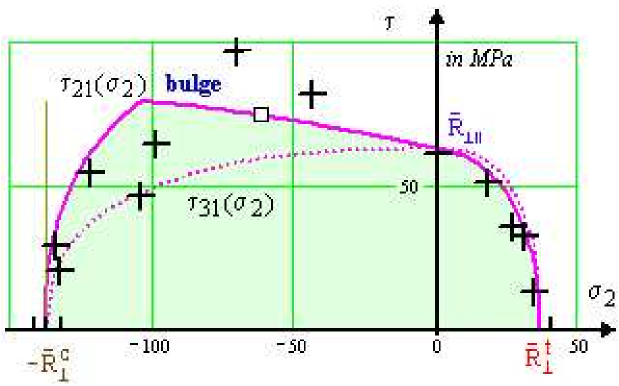

Fig. 5AB. Biaxial failure stress envelope (τ_{21},σ_2) and (τ_{31},σ_2). UD-lamina (no curing stress). GFRP: E-glass/LY556 epoxy. Eq(1, 23). Test data[8] of tube **+.** $b_{\perp\parallel}=0.30,\ b^\tau_{\perp\parallel}=0,\ \dot{m}=2.5$; $b_{\perp\parallel}$-calibration in □, see Part A[14]. $\{\bar{R}\} = (1140,\ 570,\ 36,\ 138,\ 63)^T$

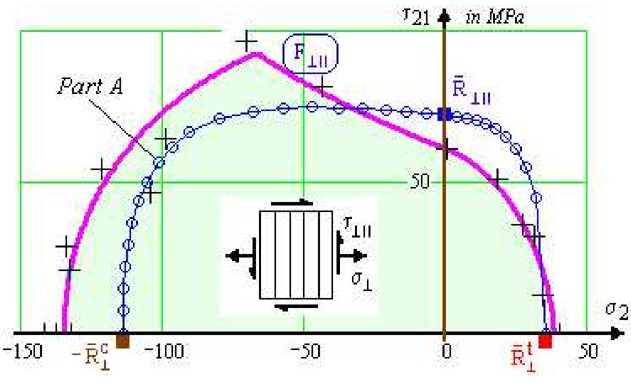

Fig. 5B with **A**. (TC1). Eqs(1 or 16, and 23). 'Blind' data: $b_{\perp\parallel}=0.13,\ b^\tau_{\perp\parallel}=0.4,\ \dot{m}=3.1$; $b^\tau_\perp = 1.5, \{\bar{R}\} = (1140,\ 570,\ 35,\ 114,\ 72)^T$.

Eq(23) applied in all figures Assumed 'best fit data set': $b_{\perp\parallel}=0.56,\ b^\tau_{\perp\parallel}=0,\ \dot{m}=2.1,\ b^\tau_\perp = 1.09$ $\{\bar{R}\} = (1140,\ 570,\ 38,\ 135,\ 62)^T.(1 \equiv \parallel,\ 2 \equiv \perp)$. *MaxTau =105 MPa.* In all other TCs an identical data set is used for the material.

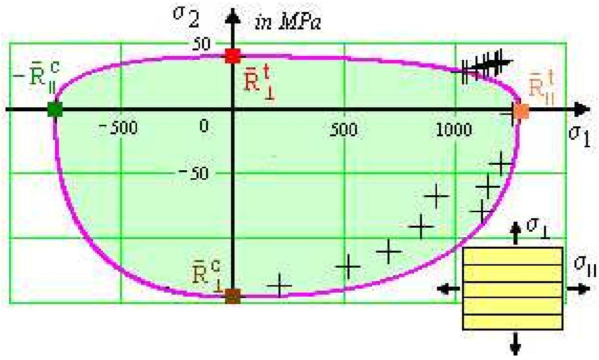

Fig. 7. (TC3) Biaxial failure stress envelope $(\sigma_{2,}, \sigma_1)$. UD-lamina. E-glass/MY750epoxy[3]. Eqs(1, Part A or 16, Part B). Hoop wound tube data[8] **+**, $\dot{m} = 3.1$. $\{\bar{R}\} = (1280, 800, 40, 145, 73)^T$, $\sigma_1 = \sigma_{hoop}$, $\sigma_2 = \sigma_{axial}$ ($b_\perp^\tau = 1.5$, $b_{\perp\parallel} = 0.13$, $b_{\perp\parallel}^\tau = 0.4$ just for information).

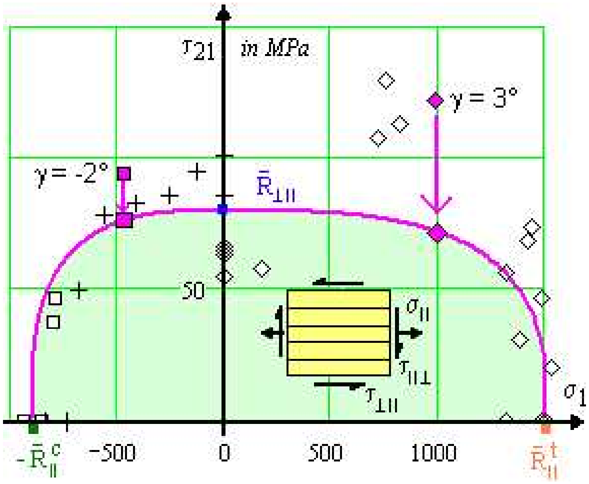

Fig. 6. (TC2) .Eqs(1or16). Biaxial failure stress envelope (τ_{21}, σ_2) in MPa. UD-lamina T300/BSL914C epoxy [3]. Axially wound Tube. Eq(1 or 16). $\dot{m} = 3.1$ $\{\bar{R}\} = (1500, 900, 27, 200, 80)^T$. Corrected test data due to computed shear deformation γ: ■◆. Transformation of ($\sigma_x \equiv \sigma_1$, $\sigma_y \equiv \sigma_2$, $\tau_{yx} \equiv \tau_{21}$) into real lamina stresses ($\sigma_\parallel, \sigma_\perp, \tau_{\perp\parallel}$). Assumed curve parameters $b_{\perp\parallel} = 0.13$, $b_{\perp\parallel}^\tau = 0.4$, $b_\perp^\tau = 1.5$ (Eq(1) have no influence.

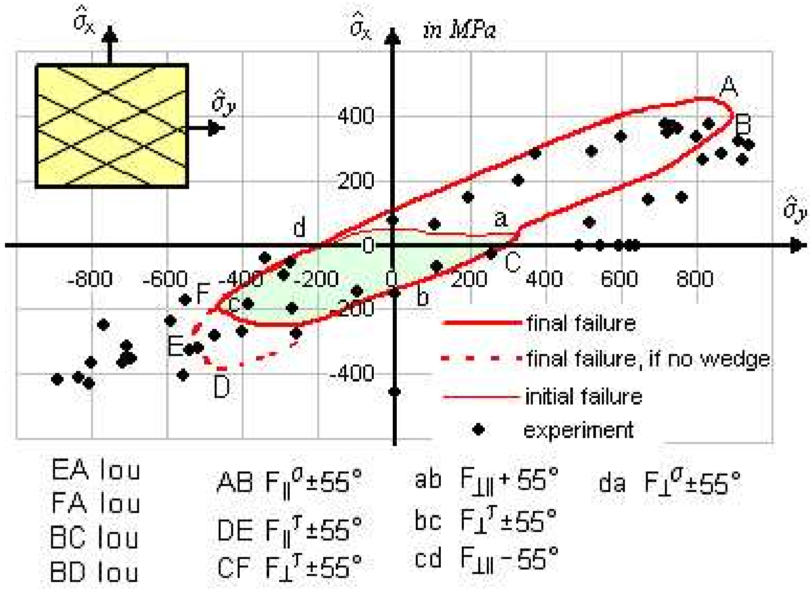

Fig. 8A (TC9) Initial and final failure envelope $\hat{\sigma}_y(\hat{\sigma}_x)$. Filament wound tube,[+55/-55/55/-55]-laminate, E-glass/MY750 epoxy[3] Eq(1): $\dot{m} = 3.1$, $b_\perp^\tau = 1.5$, $b_{\perp\parallel} = 0.13$, $b_{\perp\parallel}^\tau = 0.4$.

$\hat{\sigma}_y$:= average hoop stress of the laminate, x:= $0°$ direction. Limit of usage (lou) at $\gamma = 4\%$.

Fig. 9A. (TC5) Initial and final biaxial failure envelope $\hat{\tau}_{xy}(\hat{\sigma}_x)$. [90/+30/-30/30/-30/90]-laminate. E-glass/LY556 epoxy[3]. $\hat{\sigma}_x$ is parallel to 0°-direction. Filament wound tube test data[8] ΔT=-68°C; $b_\perp^\tau = 1.5$, $b_{\perp\parallel} = 0.13$, $b_{\perp\parallel}^\tau = 0.4$, Eq(1), $\dot{m} = 3.1$. $\{\bar{R}\} = (1140, 570, 35, 114, 72)^T$.

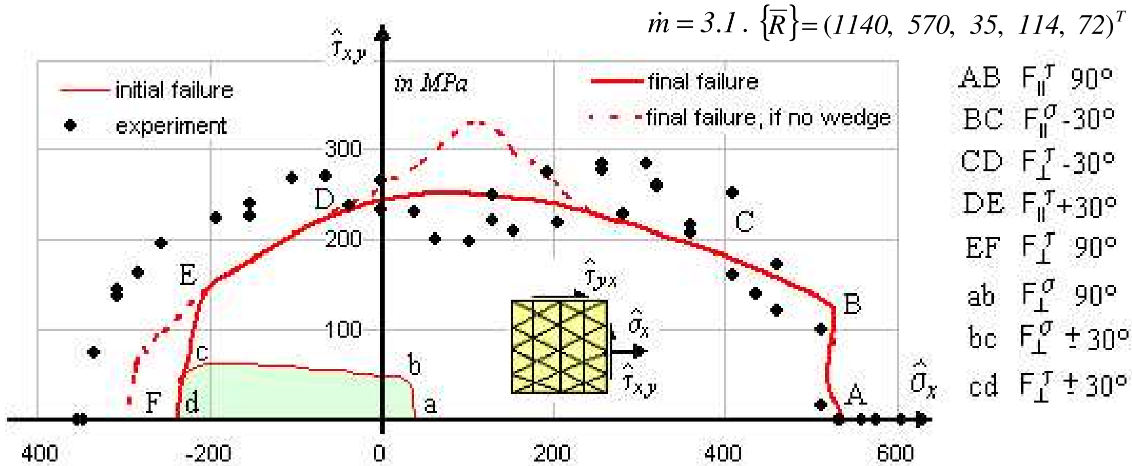

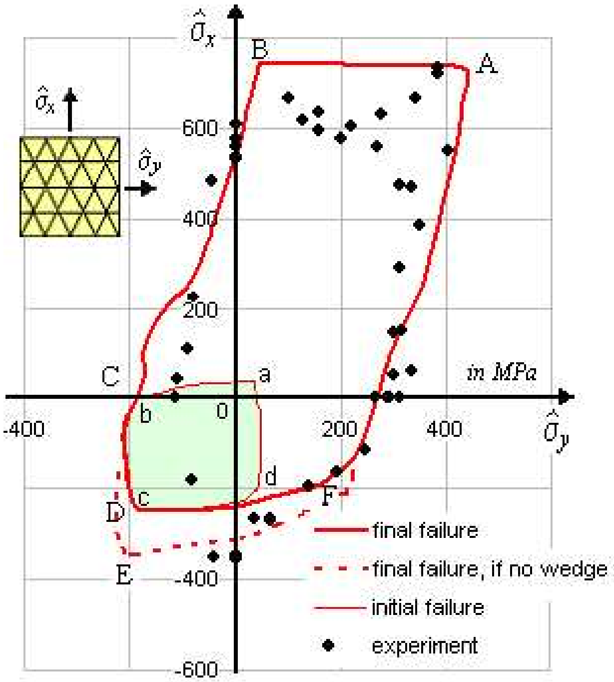

ab $F_\perp^\sigma$ 90° AB $F_\parallel^\sigma$ ± 30° DF $F_\perp^\tau$ 90°
bc $F_\perp^\tau$ ± 30° BC $F_\parallel^\tau$ 90° EF $F_\parallel^\tau$ ± 30°
cd $F_\perp^\tau$ 90° BE $F_\parallel^\tau$ 90° FA $F_\parallel^\sigma$ 90°
da $F_\perp^\sigma$ ± 30° CD $F_\perp^\tau$ ± 30°

Fig. 10A. (TC4) Initial and final biaxial failure envelope $\hat{\sigma}_y(\hat{\sigma}_x)$. [90/30/-30/30/-30/90]-laminate. E-glass/LY556 epoxy[3]. Hoop wound tube, liner. Eq(1), $b_\perp^\tau = 1.5$, $b_{\perp\parallel} = 0.13$, $b_{\perp\parallel}^\tau = 0.4$, $\dot{m} = 3.1$. $\{\bar{R}\} = (1140,\ 570,\ 35,\ 114,\ 72)^T$.

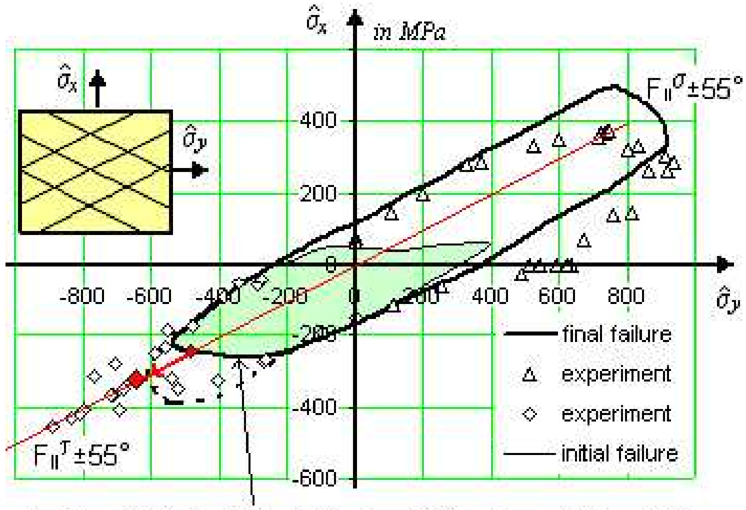

ab $F_{\perp\parallel}$ + 55° bc $F_\perp^\tau$ ±55° da $F_\perp^\sigma$ ±55° cd $F_{\perp\parallel}$ - 55°

Fig. 8B. (TC9) Initial and final failure envelope $\hat{\sigma}_y(\hat{\sigma}_x)$. [+55/-55/55/-55]-laminate, E-glass /MY750 epoxy[3]. Filament wound tube test data[8].: ΔT= -68°C, $\{\bar{R}\} = (1280,\ 800,\ 40,\ 145,\ 73)^T$, $\dot{m}$ = 3.1, new $F_\perp^\tau$ (Eq(16)□ $newb_\perp^\tau = 1.09$, $b_{\perp\parallel}^\tau = 0.4$, $b_{\perp\parallel} = 0.13$. Bulging reported in experiment. Limit of usage (lou) at $\gamma = 10\ \%$. Dashed curve: final failure of a full wedge failure-insensitive stack.
◆ corrected value.

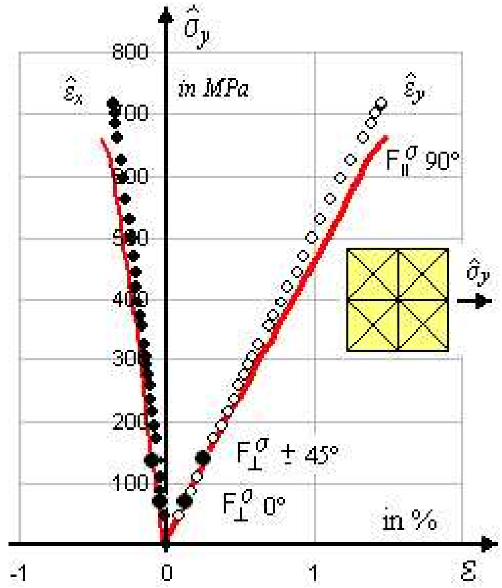

Fig. 11A. (TC7) Stress-strain curves. Eq(1). $\hat{\sigma}_y : \hat{\sigma}_x = 1:0$. $[0/+45/-45/90]_S$-laminate AS4/3501-6 epoxy. Hand lay-up cylinder. $\{\bar{R}\} = (1950,\ 1480,\ 48,\ 200,\ 79)^T$.

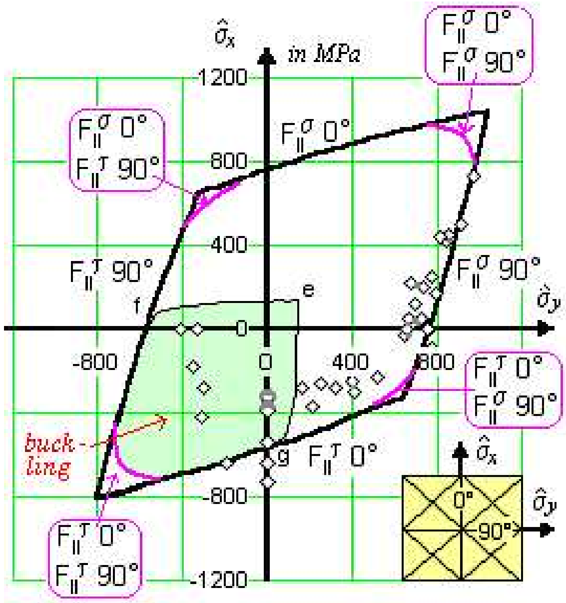

ge $F_\perp^\sigma$ 0°, ef $F_\perp^\sigma$ 90°

Fig. 12B. (TC6) Initial and final failure envelope $\hat{\sigma}_y(\hat{\sigma}_x)$. $[0/45/-45/90]_s$-laminate, AS4/3501-6 [3]. $\hat{\sigma}_y$: = average hoop stress of the laminate, x:=0° direction. ΔT= -125°C. Hand lay-up cylinder. Test data[8]: $newb_\perp^\tau = 1.09$, $Eq(16)$, $b_{\perp\parallel} = 0.13$, $\dot{m} = 3.1$; $\{\bar{R}\} = (1950,\ 1480,\ 48,\ 200,\ 79)^T$. Rounding by joint failure probability of adjacent laminae, estimated

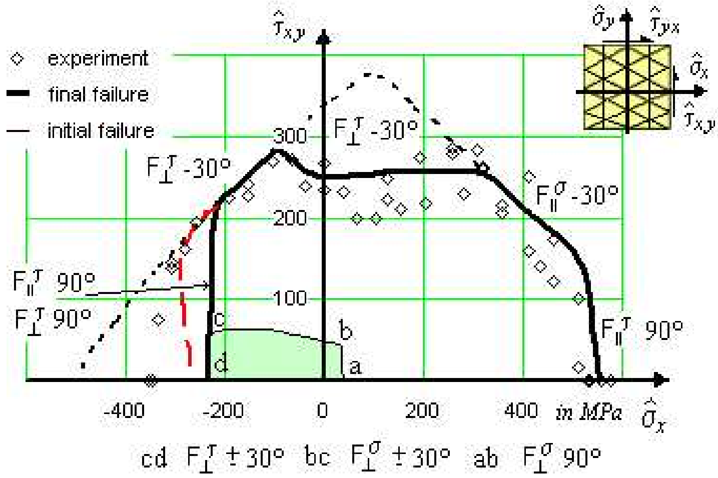

Fig. 9B with Improvement. (TC5) Initial and final bi-axial failure envelope $\hat{\tau}_{xy}(\hat{\sigma}_x)$. [90/+30/-30]$_n$ -laminate. E-glass/LY556 epoxy[3]. $\hat{\sigma}_x$ is parallel to 0°-direction. Test data[8]: ΔT= -68°C. $\{\bar{R}\}=(1140,\ 570,\ 35,\ 114,\ 72)^T$. $newb_\perp^\tau = 1.09\ Eq(16),\ b_{\perp\parallel} = 0.13,\ \dot{m} = 3.1$. Dashed line: increase due to $\bar{R}_\perp^c = 114 \Rightarrow 138MPa$.

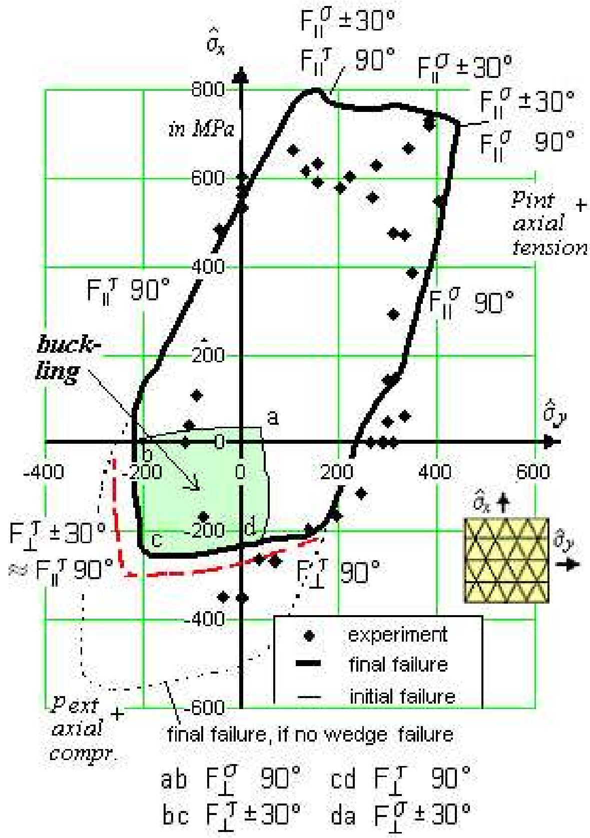

Fig. 10B. (TC4) Initial and final biaxial failure envelopes $\hat{\sigma}_y(\hat{\sigma}_x)$. [90/+30/-30]$_n$-laminate (n varies between 1 and 4). E-glass/LY556 epoxy[3]. ΔT= -68°C. Tube Test data[8]:
$\{\bar{R}\}=(1140,\ 570,\ 35,\ 114,\ 72)^T$.
$newb_\perp^\tau = 1.09\ Eq(16),\ b_{\perp\parallel} = 0.13,\ \dot{m} = 3.1$.

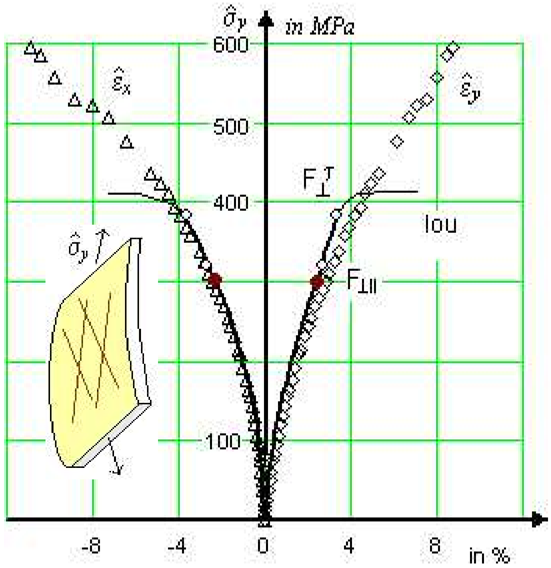

Fig 13B with **A.** (TC10) Stress-strain curves for $\hat{\sigma}_y{:}\hat{\sigma}_x = 1{:}0$ *(radial loading by p_{int} + axial compression load).* Tube, [+55/-55/55/-55]-laminate, E-glass/MY750[3]; Test data[8]: ΔT= -68°C. $newb_\perp^\tau = 1.09\ Eq(16);\ b_{\perp\parallel} = 0.13;\ \dot{m} =$ 3.1, $\{\bar{R}\} = (1280,\ 800,\ 40,\ 145,\ 73)^T$, $max\gamma = 10\ \%$. $\hat{\sigma}_y = \sigma_{hoop}$. Final Part A point●.

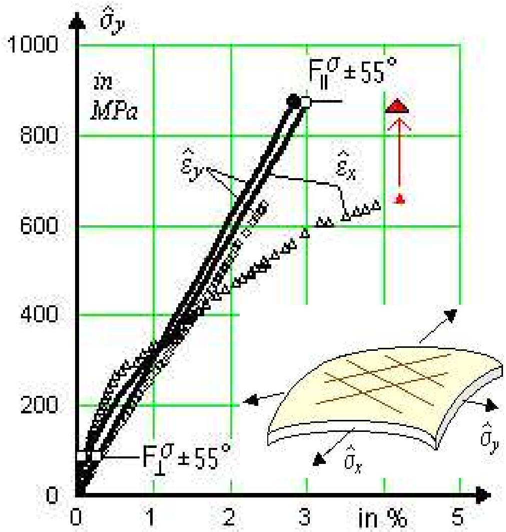

Fig. 14B with **A.** (TC11) Stress-strain curves for $\hat{\sigma}_y{:}\hat{\sigma}_x = 2{:}1$ (p_{int}), [+55/-55/55/-55]-laminate. E-glass / MY750 [3].ΔT= -68°C. Test data[8]. Corrected maximum test values. Final Part A point●. $\hat{\sigma}_y = \sigma_{hoop}$, $\{\bar{R}\} = (1280,\ 800,\ 40,\ 145,\ 73)^T$.

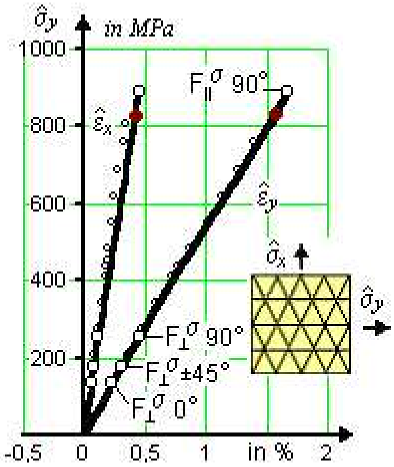

Fig. 15B with **A.** (TC8) Stress-strain curves for $\hat{\sigma}_y:\hat{\sigma}_x = 2:1$ *(p_{int})*. $[0/+45/-45/90]_S$-laminate. Tube test data[8]. AS4/3501-6 epoxy. ΔT= -125°C. Final Part A point●. $\{\overline{R}\} = (1950,\ 1480,\ 48,\ 200,\ 79)^T$. No curve parameters necessary.

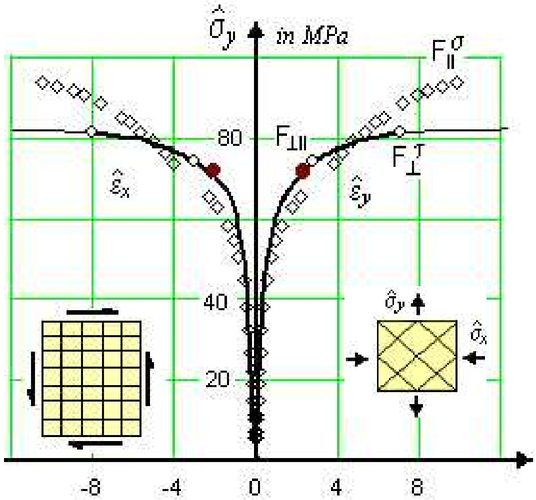

Fig. 16B with **A.** (TC14) Stress-strain curves for $\hat{\sigma}_y:\hat{\sigma}_x = 1:-1$ *(shear by p_{int} + axial compression)* .[+45/-45/45/-45]-laminate. E-glass/MY750[3]. ΔT = -68°C. Tube test data[8]. Bulging reported in experiment. $\hat{\sigma}_y = \sigma_{hoop}$. Final Part A point●.

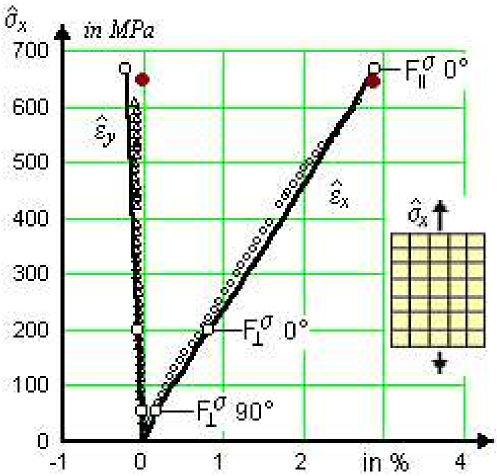

Fig. 17B with **A.** (TC12) Stress-strain curves for $\hat{\sigma}_y:\hat{\sigma}_x = 0:1$, *(axial tension)*. $[0/90]_S$-laminate. Coupon!. E-glass/ MY750 [3]. ΔT= -68°C. Test data[8]. Final Part A point●.

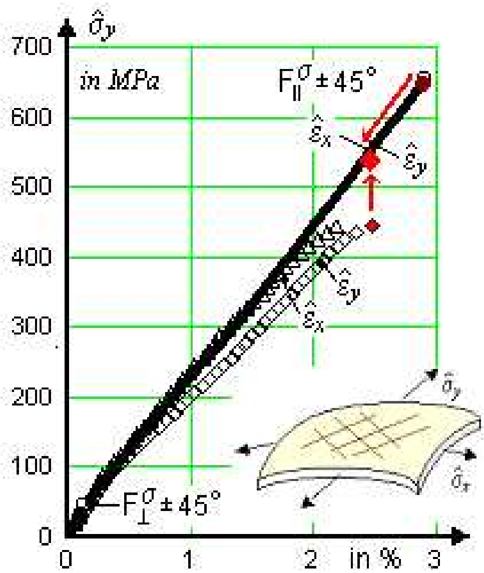

Fig. 18B with **A.** (TC13) Stress-strain curves for $\hat{\sigma}_y:\hat{\sigma}_x = 1:1$, *($p_{int}$ + axial tension)*.[+45/-45/45/-45]-laminate. E-glass/MY750 [3]. ΔT= -68°C. Tube test data[8]. Bulging reported in experiment. ◆ maximum test value after two corrections. $\hat{\sigma}_y = \sigma_{hoop}$ .Final Part A point●. $\{\overline{R}\} = (1280,\ 800,\ 40,\ 145,\ 73)^T$

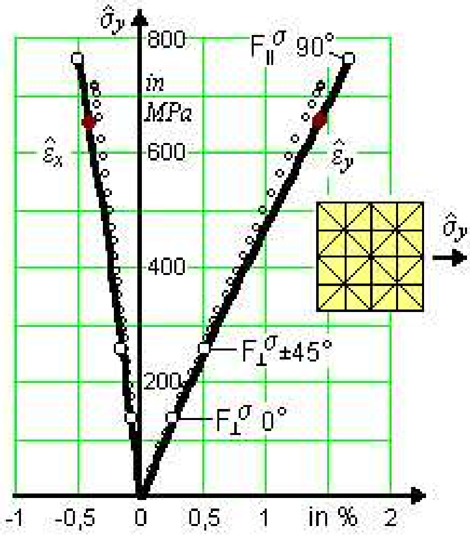

Fig. 11B with **A.** (TC7) Stress-strain curves for $\hat{\sigma}_y:\hat{\sigma}_x = 1:0$. *(radial loading induced by p_{int} + axial compression)*. $\hat{\sigma}_y = \sigma_{hoop}$ $[0/+45/-45/90]_S$-laminate. AS4/3501-6/ epoxy[3]. $\{\overline{R}\} = (1950,\ 1480,\ 48,\ 200,\ 79)^T$. ΔT=-125°C. Test data[8]. Final Part A point●.

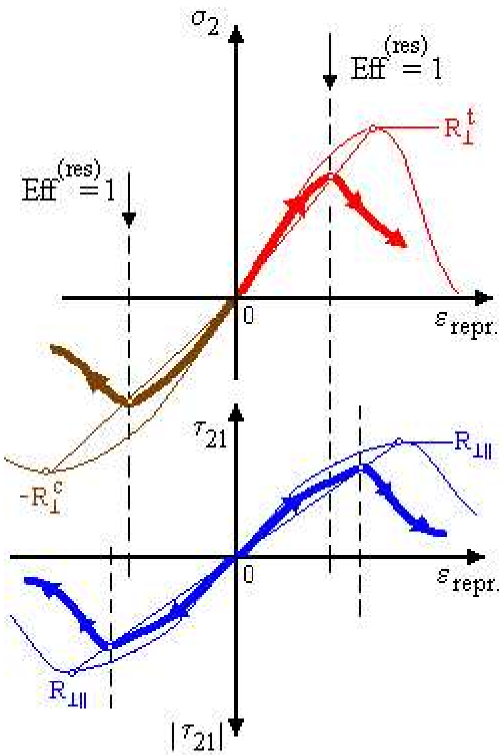

Fig. 19. Schematic illustration of Cuntze's assumptions about the stresses σ_2 and τ_{21} before and after IFF-initiation. Over-pronounced results of the 'triggering approach'.

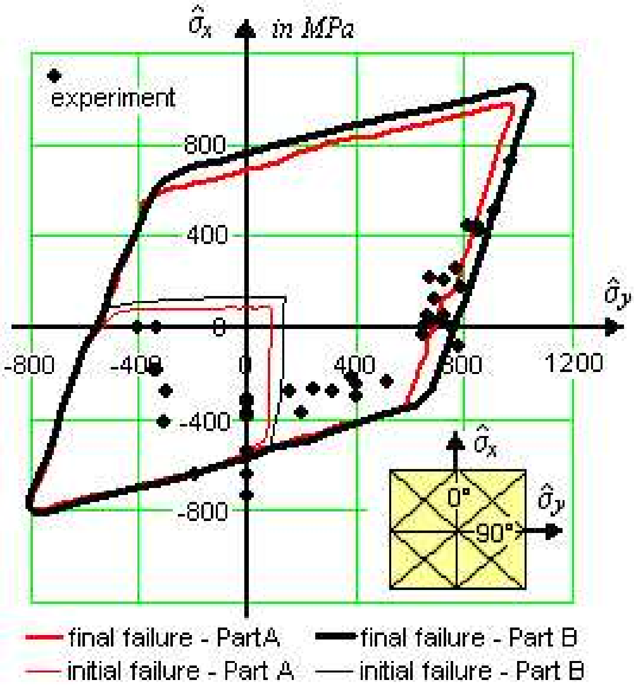

Fig. 12B with **A.** (TC6) Initial and final failure envel. $\hat{\sigma}_y(\hat{\sigma}_x)$ in MPa. $[0/45/-45/90]_S$-laminate, AS4/3501-6 [3].

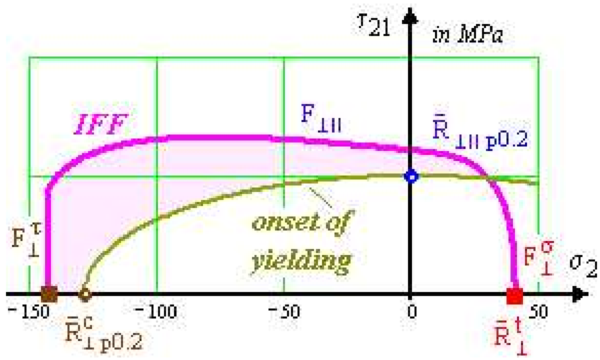

Fig. 20a. Yielding zone (shadowed) in the (τ_{21}, σ_2) domain

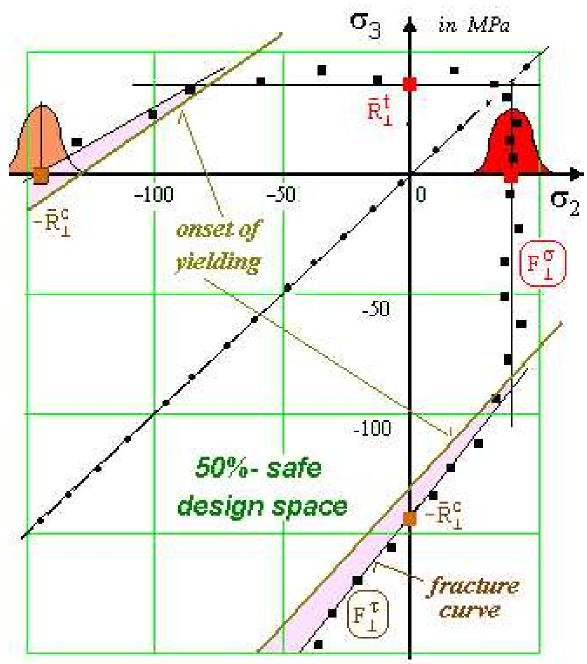

Fig. 20b. Yielding zone in the (σ_3, σ_2) domain (rounding-off intentionally not applied)

Table 1. Different meanings of theoretical and experimental data

	Theory CLT (plane)	**Experiment** tube effect
$\hat{\sigma}_x, \hat{\sigma}_y$	actual laminate, mean stresses	basis: small strains
$\hat{\varepsilon}_x, \hat{\varepsilon}_y$	large strains	large strains
	no tube effect $\rightarrow$ no large deform.	tube effect $\rightarrow$ large deformation
	no tube effect $\rightarrow$ bulging missing	tube effect $\rightarrow$ bulging included
	-	creep??